Science of the Total Environment 800 (2021) 149535

Contents lists available at ScienceDirect

Science of the Total Environment

journal homepage: www.elsevier.com/locate/scitotenv

Comprehensive assessment of MODIS-derived near-surface air temperature using wide elevation-spanned measurements in China

Wenjie Zhang [a,b], Baiping Zhang [b], Wenbin Zhu [b,*], Xiaolu Tang [c,d], Fujie Li [e], Xisheng Liu [f], Qiang Yu [b,g]

[a] Collaborative Innovation Center on Forecast and Evaluation of Meteorological Disasters, School of Geographical Sciences, Nanjing University of Information Science & Technology, Nanjing 210044, China
[b] Institute of Geographic Sciences and Natural Resources Research, Chinese Academy of Sciences, Beijing 100101, China
[c] College of Ecology and Environment, Chengdu University of Technology, Chengdu 610059, China
[d] State Environmental Protection Key Laboratory of Synergetic Control and Joint Remediation for Soil & Water Pollution, Chengdu University of Technology, Chengdu 610059, China
[e] Chinese Research Academy of Environmental Sciences, Beijing 100012, China
[f] Hydrology and Water Resources Survey Bureau of Qinghai Province, Xining, China
[g] School of Life Sciences, University of Technology Sydney, Sydney, NSW, Australia

HIGHLIGHTS

- MODIS-derived near-surface air temperature using four methods are compared in China.
- Elevation and clouds have significant impact on the performance of different methods.
- Hydrostatic interpolation can solve the underestimation issue in high elevation area.
- Averaging with land surface temperature reduces the elevation and cloud effects.
- This study will provide important references for future use in global models.

GRAPHICAL ABSTRACT

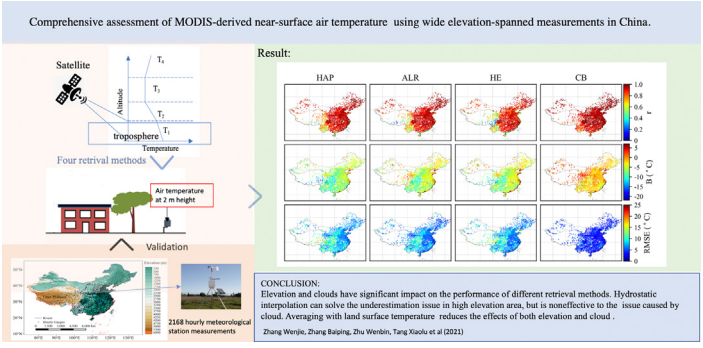

ARTICLE INFO

Article history:
Received 21 March 2021
Received in revised form 3 August 2021
Accepted 4 August 2021
Available online xxxx

Editor: Pavlos Kassomenos

Keywords:
Atmospheric profile product
Interpolation
The highest available pressure
Adiabatic lapse rate
Hypsometric equation

ABSTRACT

This is the first comprehensive evaluation of the Moderate Resolution Imaging Spectroradiometer (MODIS)-derived near-surface air temperature, which has been used widely in a series of large-scale models varying in various disciplines ranging from climatology, hydrology to ecology. Four retrieval methods: the highest available pressure in the atmospheric profile product, interpolation by the adiabatic lapse rate, interpolation by the hypsometric equation and the combination with land surface temperature, were developed in the past, but only with validation in regional scale. All of these are evaluated in this paper against 2168 hourly meteorological recordings with an elevation span of over 5000 m in China. Results show that the method of the highest available pressure exhibits a serious underestimation, especially in areas of high elevation, such as the Tibetan Plateau. Interpolation by the hypsometric equation can only fix the underestimation to a very small extent, while interpolation by the adiabatic lapse rate can achieve a relatively good performance. In addition to the elevation influence, substantially variable estimates occur with the parabola-like distribution in low elevation areas, which implies the influence of cloud in Southern China. The combination of the underestimation from interpolation by the adiabatic lapse rate and overestimation in land surface temperature can eliminate the disturbance of both elevation and cloud, resulting in the best performance with r = 0.94, bias = −0.83°C and root-mean-square-error = 4.18°C.

* Corresponding author at: Institute of Geographic Sciences and Natural Resources Research, Chinese Academy of Sciences, Beijing, China.
E-mail address: zhuwb@igsnrr.ac.cn (W. Zhu).

https://doi.org/10.1016/j.scitotenv.2021.149535
0048-9697/

1. Introduction

Near-surface air temperature (T_a), typically measured at the shelter height of 2 m above ground, is an important descriptor of terrestrial environmental conditions across the earth (Monteith, 1973; Sellers et al., 1997). It controls many biological and physical processes between the earth surface and the atmosphere, including respiration, transpiration, and photosynthesis (Nieto et al., 2011; Prihodko and Goward, 1997; Zveryaev et al., 2016). T_a is one of the most routine elements observed at meteorological stations (Stisen et al., 2007). However, the uneven distribution of these measurements has limited the ability to reflect the spatial heterogeneity of T_a (Geiger, 1965).

Over the past few decades, remote sensing (RS) techniques have proven to be a sound alternative to provide spatially distributed T_a information (Shen and Leptoukh, 2011; Sun et al., 2005; Zhang et al., 2015; Zhu et al., 2013). Compared with T_a estimation during the night, the retrieval of T_a from RS observations during daytime is far from straightforward due to the complex interaction of the surface energy balance system (Golkar et al., 2018; Vancutsem et al., 2010). In order to obtain a better estimation of T_a during daytime, most of the previous retrieval of T_a from RS is based on the correlation between T_a and remotely sensed land surface temperature. According to the review of Liu et al. (2017), these previous parameterization schemes can be broadly classified into three types including the simple and advanced statistical approaches (Cristóbal et al., 2008; Lin et al., 2012; Peón et al., 2014), the Temperature-Vegetation index (TVX) method (Goward et al., 1994; Nieto et al., 2011; Stisen et al., 2007; Zhu et al., 2013), and algorithms based on the surface energy balance principle (Benali et al., 2012; Mostovoy et al., 2006; Prince et al., 1998). Geostatistical methods also can be used to estimate T_a from the combination of elevation and land surface temperature (Collados-Lara et al., 2021). The accuracy of these methods has been evaluated in a large number of studies across the world (Cai et al., 2017; Liu et al., 2017; Oyler et al., 2016). In general, daytime T_a estimates with high accuracy can only be achieved by adopting in-situ meteorological observations as an auxiliary.

To reduce the reliance on ground measurements, several studies have attempted to retrieve T_a from MODIS atmosphere profile products in recent years (Bisht and Bras, 2010; Jang et al., 2014; Kim and Hogue, 2008; Zhu et al., 2017b). A simple summary of such studies can be found in the research of Zhu et al. (2017b) and Famiglietti et al. (2018). Specifically, the MODIS Level-2 atmospheric profile product (MOD07) provides atmosphere temperature distributed at 20 vertical atmospheric pressure levels. The vertical atmosphere temperature profile makes it possible to predict T_a based on hydrostatic assumptions without the need for in-situ measurements (Bisht and Bras, 2010; Zhu et al., 2017a; Zhu et al., 2017b). However, previous studies have only been performed on regional scales (Hu and Brunsell, 2015; Jang et al., 2013; Sobrino et al., 2015). Although recently the accuracy of near-surface T_a retrieved from MOD07 has been validated at a global scale by Famiglietti et al. (2018), the low density of ground meteorological stations (only 109 FLUXNET stations) in their study may result in a loss of some key information. Up until now, there have been at least four parameterization schemes to estimate T_a from the MOD07 product, however, only one of these has been validated in the research of Famiglietti et al. (2018). More importantly, the T_a estimates for validation in their research were produced through a linear regression approach using the in-situ T_a observations as input. To some extent this contradicts the original intention of such parameterization schemes because the retrieval of T_a from MOD07 in previous studies was designed in general to avoid the need for ancillary ground observations. Therefore, a large-scale and comprehensive evaluation of different parameterization schemes of T_a from MOD07 product is still absent, making the quality of the retrievals at the heights relevant for many modeling applications unclear (Ryu et al., 2011; Seddon et al., 2016; Verma et al., 2016).

The objective of this study is to present a comprehensive evaluation of four different parameterization schemes and gain an understanding how well T_a can be retrieved from the MOD07 product without ancillary of in-situ observations. The accuracy of T_a estimates is validated with data collected from 2168 hourly meteorological station measurement across mainland China from 2017. A full characterization of the accuracies over the large-scale, including regional trends, seasonal variability, and their related influencing factors, provides valuable insights into the reliability of these different parameterization schemes.

2. Material and methods

2.1. Near-surface air temperature retrieved from the atmospheric profile product

MOD07 temperature profiles consist of atmosphere temperatures distributed at 20 vertical atmospheric pressure levels (5, 10, 20, 30, 50, 70, 100, 150, 200, 250, 300, 400, 500, 620, 700, 780, 850, 920, 950, and 1000 hPa). Based on a review of previous studies, four T_a parameterization schemes from MOD07 product are evaluated in this study. It should be noted that all of these four parameterization schemes are developed based entirely on MODIS products without any ancillary ground observations.

2.1.1. Near-surface air temperature from the highest available pressure level

MOD07 provides air temperature profiles at 20 vertical pressure levels. In theory, the T_a observations from the highest available pressure level (HAP) have the potential to be used directly as the proxy for T_a (Bisht et al., 2005; Seddon et al., 2016). The mathematical formula of HAP method is expressed as:

$$T_{a,HAP} = T_a^{H1} \tag{1}$$

where $T_{a,\,HAP}$ represents T_a retrieved by HAP, and T_a^{H1} represents the atmosphere temperature of the highest available pressure level of MOD07.

2.1.2. Interpolation by the adiabatic lapse rate

In order to reduce the uncertainty caused by the pressure difference, several new parameterization schemes of T_a have been proposed based on the hydrostatic atmospheric assumption of the troposphere (Bisht and Bras, 2010; Flores and Lillo, 2010). The parameterization scheme proposed by Zhu et al. (2017b) is used in this study as a representative. Firstly, the adiabatic lapse rate (ALR) is retrieved from the two highest available pressure levels of MOD07 as follows:

$$ALR = \frac{T_a^{H2} - T_a^{H1}}{\Delta H} = \rho g \frac{T_a^{H2} - T_a^{H1}}{P^{H2} - P^{H1}} \tag{2}$$

where ΔH is the height difference between the two highest available pressure levels, ρ is the density of the air, g is the gravitational acceleration, P^{H2} is the nearest pressure level lower than P^{H1}, and T_a^{H2} is the corresponding atmosphere temperature of P^{H2}.

Applying the ALR retrieved above to surface pressure level (P^S), T_a is estimated as:

$$T_{a,ALR} = T_a^{H1} + \frac{ALR}{\rho g}\left(P^S - P^{H1}\right) = T_a^{H1} + \frac{T_a^{H2} - T_a^{H1}}{P^{H2} - P^{H1}} \times \left(P^S - P^{H1}\right) \tag{3}$$

where $T_{a,\,ALR}$ represents T_a retrieved by $T_{a,\,ALR}$ method.

2.1.3. Interpolation by the hypsometric equation

As interpreted above, MOD07 can provide atmosphere temperature profiles at 20 specific pressure levels. A significant difference exists between surface pressure and the highest available pressure level. To reduce the uncertainty caused by the pressure difference, a new parameterization scheme from MOD07 product has been proposed by Famiglietti et al. (2018) based on the hypsometric equation (HE).

Firstly, the distance of the surface pressure level to the two highest available pressure levels is calculated using the hypsometric equation as follows:

$$Z_1 = \frac{R}{g} \times \left(T_a^{H1} + 273.16\right) \times \log\left(\frac{P^S}{P^{H1}}\right) \quad (4)$$

$$Z_2 = \frac{R}{g} \times \left(T_a^{H2} + 273.16\right) \times \log\left(\frac{P^{H1}}{P^{H2}}\right) \quad (5)$$

where Z_1 and Z_2 are the distance of the surface pressure level (P^S) to P^{H1} and P^{H2}, respectively. R is the gas constant of dry air of 287.053 J K^{-1} kg^{-1}.

Then T_a is estimated as:

$$T_{a,HE} = T_a^{H1} + \left(T_a^{H1} - T_a^{H2}\right) \times \frac{Z_2}{Z_1} \quad (6)$$

where $T_{a,\,HE}$ represents T_a retrieved by the HE method.

2.1.4. The combination with land surface temperature

The performance of ALR was evaluated by Zhu et al. (2017b) in two regions with totally different climatic conditions. Their results showed that T_a was underestimated by ALR in both of these two regions. Their research suggested that the systematic errors of T_a estimation produced by ALR method and land surface temperature (T_s) retrieved from MODIS Cloud Product (MOD06) was in completely different directions. Accordingly, in this paper, an averaging parameterization scheme is proposed to retrieve T_a from the combination of MOD07 and MOD06 products (CB) as follows:

$$T_{a,CB} = \frac{T_{a,ALR} + T_s}{2} \quad (7)$$

where $T_{a,\,CB}$ is T_a retrieved by CB method.

2.2. Validation

Hourly T_a observations from 2168 hourly meteorological station measurements across mainland China in 2017 are used for validation purposes, and this covers a wide range of elevations of 5000 m from Western Tibetan Highlands to Northeast plain (Fig. 1). Only one year's data is employed due to the difficulty of data acquisition. The Chinese National Meteorological Administration only allows less than a week for downloading data of the hourly meteorological observations, and hence only the data from 2017 is used for this study. On the other hand, although MODIS data under clear sky conditions varies in different areas (Fig. 2), the same input data for the four methods guarantees the effectiveness of validation. In addition, T_a retrieved from MOD07 is instantaneous, only T_a measured at the time that approximates most the overpass time of the Terra satellite (within 1 h) is adopted. The overall mean difference of that in this study is 15 min. Besides using the Pearson's correlation coefficient (r), we also adopt the root-mean-square-error (RMSE) and the bias (B) to assess quantitatively the accuracy of T_a retrieval.

3. Results

Fig. 3 presents the overall performance of the above four methods. The MOD07 profile under clear days over mainland China reflects how many satellite and ground values of T_a were compared at each site. (Fig. 2). Although cloud contamination is unevenly distributed spatially, the identical data inputs for each method ensures the validity of the comparison. The estimate of the HAP method shows a serious underestimation ($r = 0.89$, $B = -7.25$°C, $RMSE = 9.08$°C) with the corresponding in-situ measurements (Fig. 3 HAP). It is consistent with our expectation because the highest pressure level of MOD07 product is generally lower than the land surface pressure. The ALR method, through hydrostatic interpolation, can reduce the underestimation and improve the performance ($r = 0.88$, $B =$ -5.32°C, $RMSE =$ 7.65°C) of HAP method (Fig. 3 ALR). Like the ALR method, the HE method is designed to correct the pressure difference by the interpolation of the hypsometric equation. However, poorer accuracy is produced ($r = 0.78$, $B = -5.29$°C, $RMSE =$ 9.47°C) due to excessive outliers (Fig. 3 HE). In contrast, the CB method can minimize the underestimation and achieve the highest accuracy ($r = 0.94$, $B = -0.83$°C, $RMSE = 4.18$°C) by averaging MOD07 ($T_{a,\,ALR}$) and MOD06 (T_s) (Fig. 3CB). It is worth noting that air temperature varies significantly with the seasons, so it is necessary to explore the seasonal effects on the performance of the four methods. As expected, biases in T_a estimates of HAP, ALR and HE methods vary substantially with the seasons, reaching the absolute maximum B of −10.23, −8.08, −7.96°C and RMSE of 10.83, 8.90, 9.24°C in summer (Jun, Jul, Aug) and the absolute minimum B of −2.81, −1.51, −1.76°C and RMSE of 4.99, 4.66 and

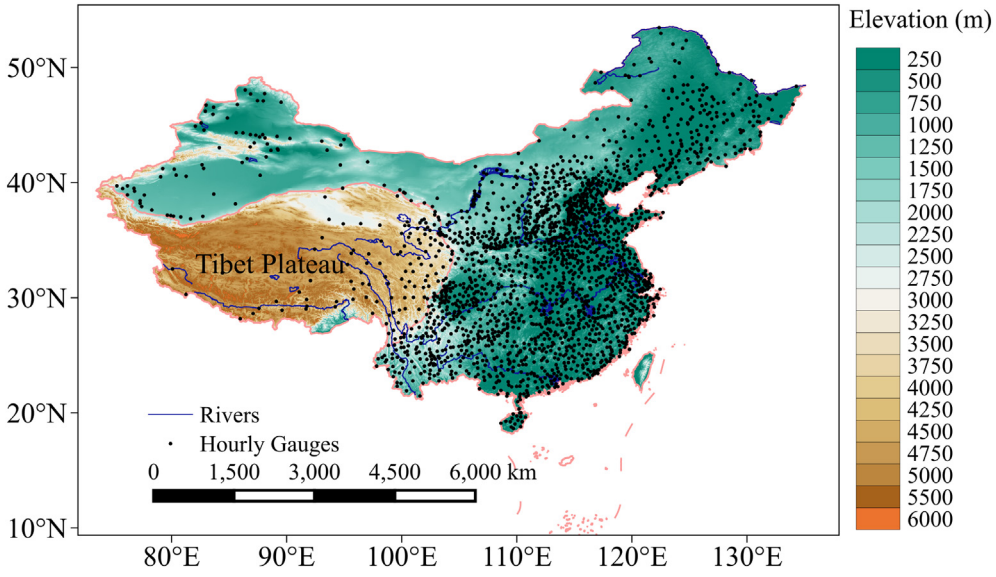

Fig. 1. The distribution of 2168 hourly meteorological stations on the elevation map of China.

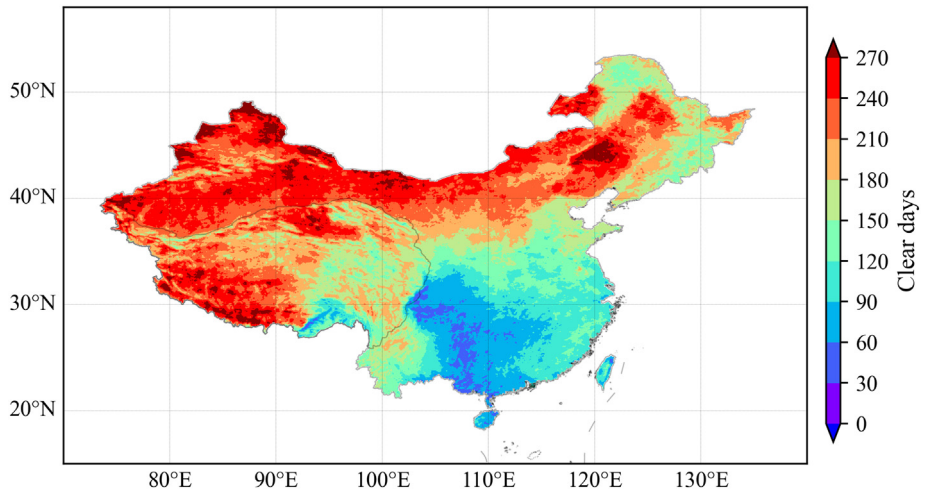

Fig. 2. Clear days of the Moderate Resolution Imaging Spectroradiometer (MODIS) Level-2 atmospheric profile product (MOD07) in 2017.

6.07°C in winter (Dec, Jan, Feb), respectively (Fig. 4). This is reasonable because the surface ground receives more solar radiation during summer, which increases the complexity of the surface energy balance system. Compared with the HAP method, both the ALR and HE methods can weaken the seasonal effects by interpolation, but the improvement was insignificant. On the contrary, the CB method tremendously ameliorated the variability in bias and achieved consistent results over all seasons (Fig. 4).

In order to investigate the spatial patterns, the errors of the above four methods are mapped using 2168 hourly meteorological station records from across China (Fig. 5). Specifically, the largest heterogeneity in errors is observed in the HAP and HE methods. Their errors as a whole decrease from the towering Tibetan Plateau to the flat eastern areas. Obviously, elevation has a significant influence on their performance. For instance, the ALR method can distinctly reduce the bias on the Tibetan Plateau (TP), which reflects its correction effect on the highest elevation area. The CB method holds the homogeneity in performance so that the above regional error propagations are overcome at the national scale. To examine the specific role of elevation in model performance, we divided all meteorological stations into 19 groups at 250 m intervals. Fig. 6 shows the different effects of elevation on the methods showing HAP and HE increasing errors over 3500 m and 2500 m respectively. However, the ALR method can significantly correct the elevation-caused errors in the large area over 3500 m apparent in

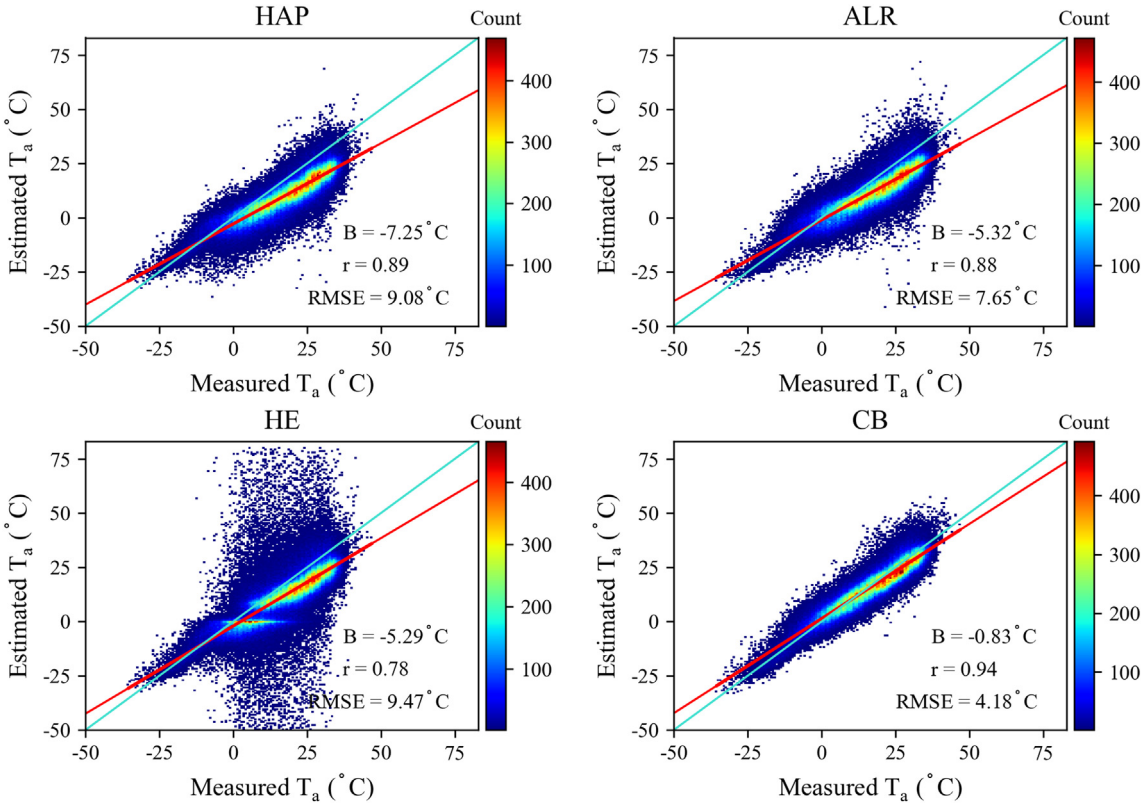

Fig. 3. Overall comparison of near-surface air temperature (T_a) estimated based on the methods of the highest available pressure in atmospheric profile product (HAP), interpolation by the adiabatic lapse rate (ALR), interpolation by the hypsometric equation (HE) and the combination with land surface temperature (CB) against 2168 hourly meteorological station records in 2017.

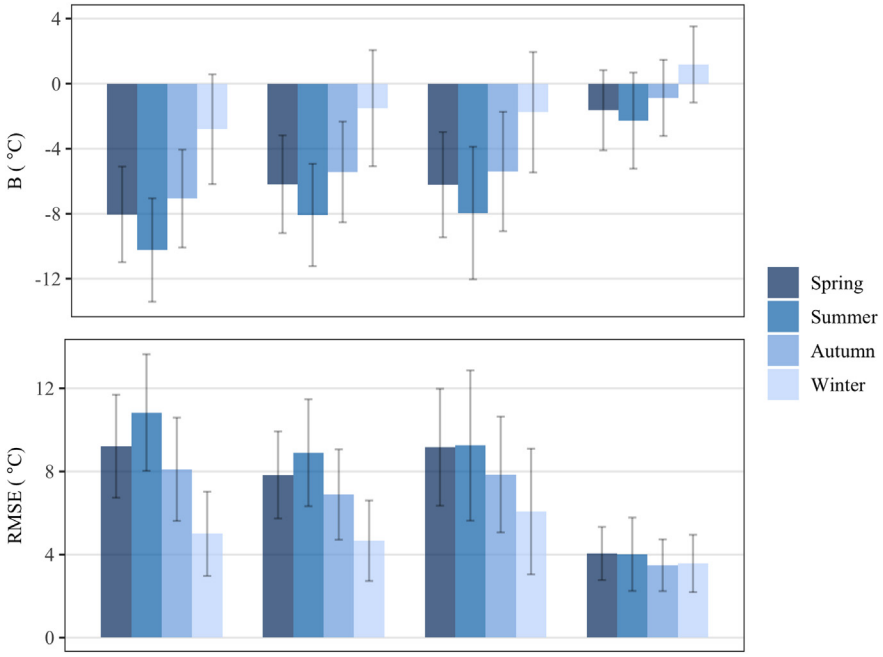

Fig. 4. Seasonal characteristics of estimate accuracy of bias (B) and root-mean-square-error (RMSE) obtained based on the methods of the highest available pressure in atmospheric profile product (HAP), interpolation by the adiabatic lapse rate (ALR), interpolation by the hypsometric equation (HE) and the combination with land surface temperature (CB). Each 4-bar represents from left to right, the results for spring, summer, fall, and winter. Spring is from March to May, others and so on.

the HAP method. Therefore, this evidence shows that the hydrostatic interpolation technique in the ALR method is superior to that adopted in the HE method for high elevation areas. Below these critical elevation thresholds, the first three methods of HAP, ALR and HE show similar parabolic error patterns reaching their negative minimum B median and positive maximum RMSE median at the 750 m group, which suggests the probable impact of clouds on accuracy (Fig. 2). Fig. 6 also indicates that the influence of elevation on model performance is diminished in the CB method. The relatively low number of stable errors when using the CB method demonstrates its validity over all elevation groups.

The annual-composited T_a demonstrates the elevation influence on the four methods especially on the TP region (Fig. 7). The severe underestimation of the HAP method leads to the abnormally cold air temperature results that is below 0 °C over most of TP. The ALR method can significantly reduce the underestimation and achieve a relatively higher accuracy, while the HE method does very little to fix this underestimation as the annual average temperature over most regions of the TP

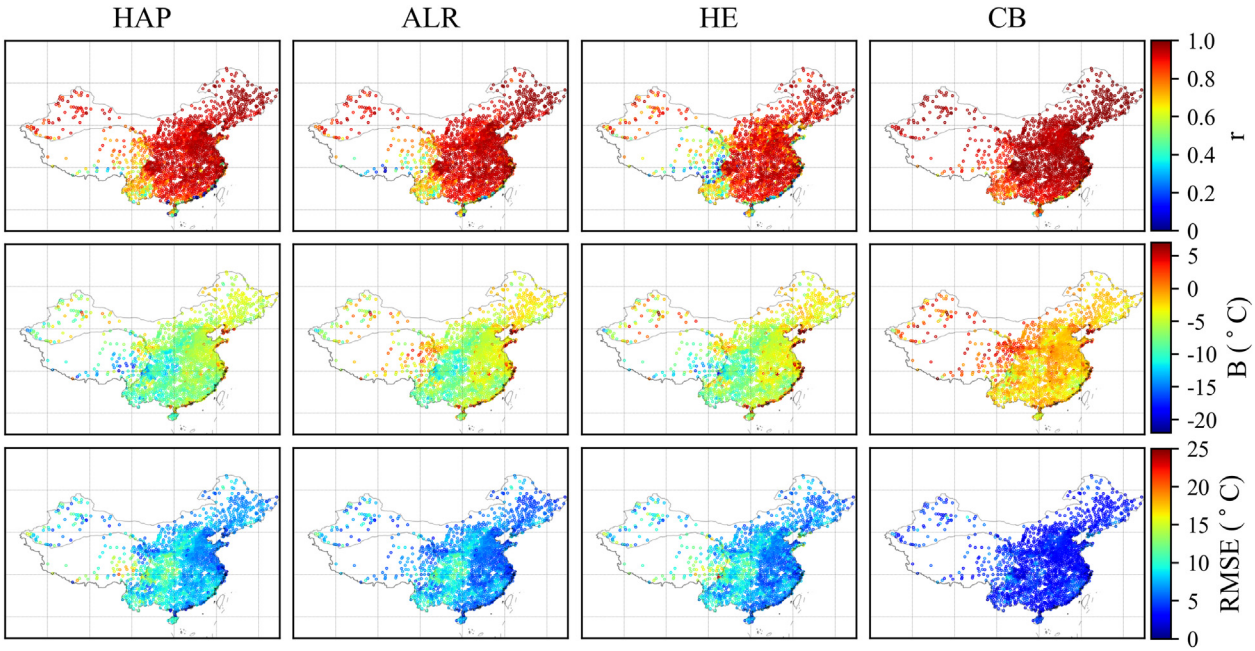

Fig. 5. Spatial distribution of the Pearson's correlation coefficient (r), bias (B) and root-mean-square-error (RMSE) statistics of estimate calculated based on the methods of the highest available pressure in atmospheric profile product (HAP), interpolation by the adiabatic lapse rate (ALR), interpolation by the hypsometric equation (HE) and the combination with land surface temperature (CB) against 2168 hourly meteorological stations in 2017 year.

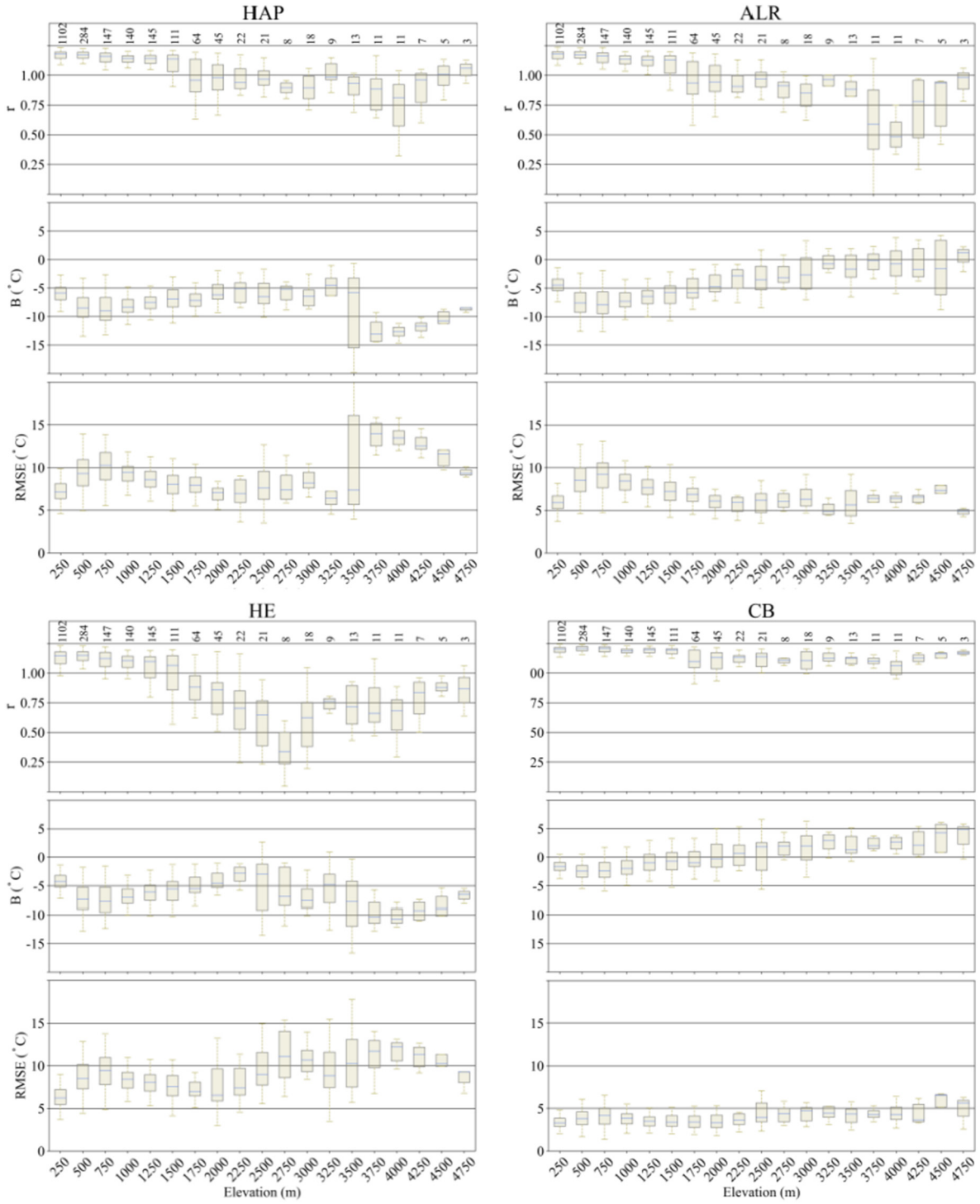

Fig. 6. Elevation-related error patterns of the Pearson's correlation coefficient (r), bias (B) and root-mean-square-error (RMSE) estimated based on the methods of the highest available pressure in atmospheric profile product (HAP), interpolation by the adiabatic lapse rate (ALR), interpolation by the hypsometric equation (HE) and the combination with land surface temperature (CB). To avoid geographical clusters of in-sites, they were divided by 250 m interval. Box heights correspond to the interquartile range, whiskers span up to 1.5 times the interquartile range, and the horizontal line corresponds to the median. The digit at the top represents the number of sites involved in the subdivision.

remains below 0°C. Compared with the methods exclusively based on the MOD07 profile, the CB method is able to correct the underestimation and thus the annual-composited T_a of more than 0°C presents over most regions of the TP.

In the CB method, due to the complementary bias between the ALR-retrieved near-surface air temperature and land surface temperature of MOD06, the averaging parameter scheme is adopted. Fig. 8 illustrates that this opposite error is widely distributed over most of the central and western regions of China. In particular, on the TP, the true proportion of the opposite error is close to 1:1. This also applies to the central region of China with coarse performance generated by the ALR method (Figs. 6 and 8). However, in the northeastern region and the eastern coastal region of China, this deviation is positive rather than negative and the reverse deviation is far from 1:1 in the southwest China region. This also implies that better results may be obtained by further correction of the ratio parameters.

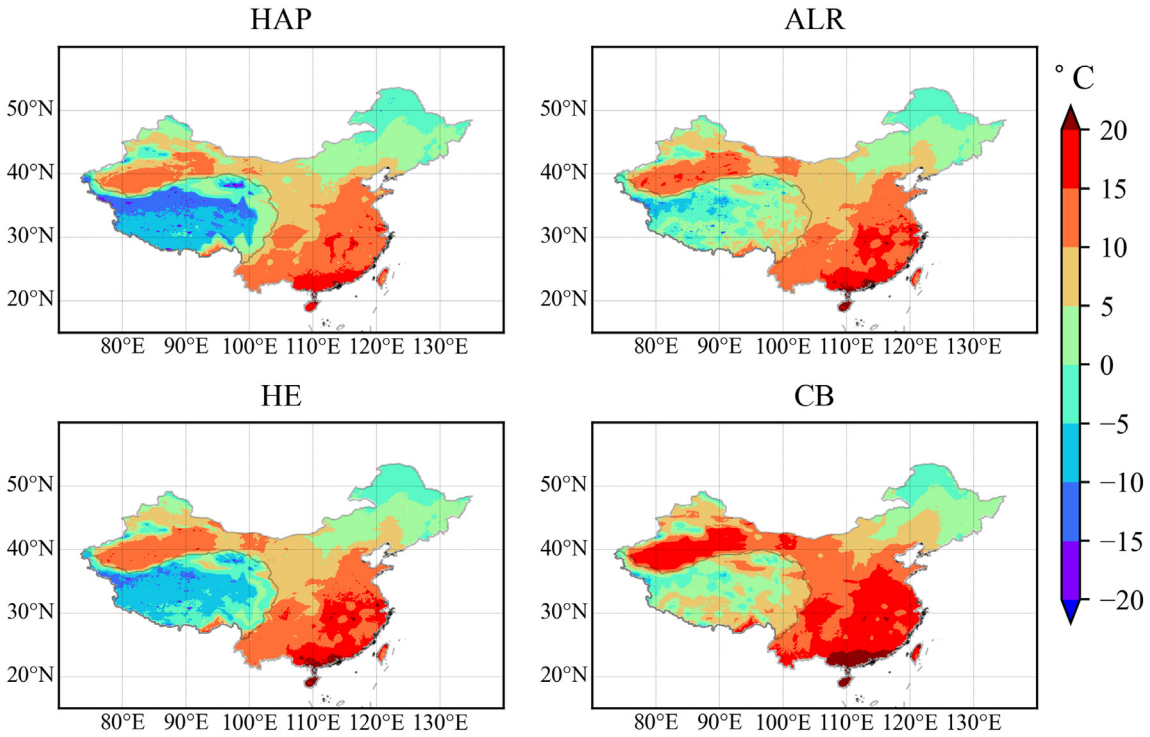

Fig. 7. Annual-integrated near-surface air temperature of 2017 that are estimated based on the methods of the highest available pressure in atmospheric profile product (HAP), interpolation by the adiabatic lapse rate (ALR), interpolation by the hypsometric equation (HE) and the combination with land surface temperature (CB).

4. Discussion

Our study shows that the accuracy of T_a estimates from MOD07 depends on both the retrieval methods used and elevation. The HAP, ALR and HE methods are developed entirely based on the MOD07, therefore, their performance can be explained by the uncertainties involved in the original data. Specifically, a clear sky global training database for hyperspectral and multi-spectral atmospheric retrievals (called BeeBor V5.0 available on https://cimss.ssec.wisc.edu/training_data/) is used for calibration in the generation of MOD07, which includes over 15,704 global profiles of temperature (Borbas et al., 2005). However, only 6% of these profiles are degrees distributed above 2000 m and 0.5% above 3500 m (Data is available on https://cimss.ssec.wisc.edu/training_data/). In addition, this implies that the temperature profile retrieved from MOD07 embodies larger uncertainty in high-elevation areas. Besides, this uncertainty might further increase in areas like the TP because of the similarity in signals between clouds and the widely-distributed glaciers and snow (Østby et al., 2014). As a result, the accuracy of the HAP method over high-elevation areas (elevation >3500 m) is worse than over low-elevation areas (elevation <3500 m). The study of Jang et al. (2014) also suggests that the performance of the HAP method for MOD07 deteriorates with the increase of elevation over the US. Furthermore, the mismatch between the highest pressure level and land surface pressure is also responsible for the serious underestimation of the HAP method. This is the basis for the development of ALR and HE methods. Apparently, the ALR method significantly

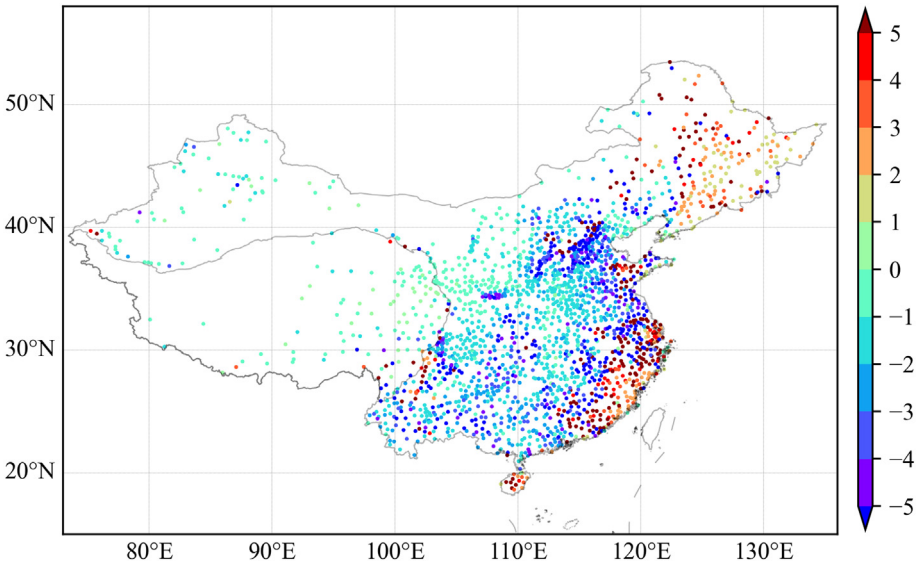

Fig. 8. The true proportion of errors retrieved from the method of interpolation by the adiabatic lapse rate against land surface air temperature on each site.

improves the performance of the HAP method by the introduction of the hydrostatic atmospheric assumption. In theory, the HE method developed from the hypsometric hypothesis is also supposed to reduce the underestimation of HAP method, however, numerous introduced outliers in return spoil the overall performance. Compared with the ALR method, the hypsometric equation is used twice in the HE method, so consequently, larger uncertainties are involved and these are particularly amplified over areas with a complex topography. A close look at Fig. 5 shows that huge errors have also arisen in low-elevation areas such as in south-central China. This indicates that errors involved in the first three methods are probably associated with other sources of uncertainty, such as cloud contamination. Fig. 2 shows the total number of days without cloud contamination in 2017. It is clear that the high incidence of cloud in the southern and central areas accounts for the low accuracy in low-elevation areas. Hu and Brunsell (2015) also conclude that cloud contamination and other factors such as sharp atmospheric structural change may result in unrealistic profiles of MOD07.

The T_a retrieved by MOD07 would have a potential application, e.g. in the global ecology-climate process model, because of its simple parameterization scheme and relatively high spatial resolution. Many studies continue to rely on the low-resolution air temperature of gridded reanalysis data such as the Climatic Research Unit (CRU) dataset as a drive (Buermann et al., 2018; Liu et al., 2018; Xie et al., 2019). However, its coarse resolution of ~0.5° (about 50 km) seriously limits the discovery of the spatially heterogeneous processes and in particular, the spatial resolution of dependent variables such as MODIS vegetation index products which achieve from 5 km to 250 m (Seddon et al., 2016; Sims et al., 2006; Zhang et al., 2017). The mismatch of the spatial resolution of dependent and independent variables in these modes has prompted the researchers to explore new climatic variables as a replacement. Hence, Seddon et al. (2016) used the daytime and nighttime temperature of the highest available pressure in MOD07 to composite monthly T_a with 5 km resolution, as one of the climatic driving in a global vegetation sensitivity model, however, it caused the loss of most TP. In our study, annual-composited T_a of HAP and HE estimates accounts for the abnormally cold air temperature over most of the TP in contrast to the results of the ALR and CB methods (Fig. 7). As a result, monthly-composited T_a of the HAP and HE methods causes the loss of the whole growing season over most of the TP because 0°C was defined as the threshold of vegetation activity. The CB method carries out the best estimations over the whole range of elevations of these methods and can guarantee a qualified ingredient for these models. We also find that the 1:1 error ratio between ALR retrievals and land surface temperature of MOD06 is not always applicable to the whole of China and further adjustment of the ratio parameters may give better results (Fig. 8).

In this paper, we specifically figured out the non-negligible role of elevation on these retrieval methods and imply their potential use with elevation-related models. However, the applicability of these methods has only been explored in China with its unique geomorphological and climatic conditions. Consequently, elevation influence on these methods' estimates still needs to be examined in the other continents considering the significant impact of the climatic condition (Famiglietti et al., 2018). In addition, because of the complex energy balance system triggered by solar radiation generally making the remote-sensing-retrieved T_a difficult (Zhu et al., 2013), much effort should be put on to assess the practicability of these methods to different sensors (Terra and Aqua) and overpass times of MODIS.

5. Conclusion

The near-surface air temperature data retrieved from the MODIS product (MOD07) offer consistent and frequent observations over large-scale areas, complementing the sparse and uneven distribution of meteorological stations across the world. However, no comprehensive assessments on the accuracy of such data from different retrieval methods have been undertaken, limiting the accurate applications of the air temperature data. This study used a novel framework to assess and quantify the differences among four MOD07-based retrieval methods over a large area with significant relief. Our results show that great impact of elevation on the retrieval outcomes from different methods. In high elevation regions, such as the Tibet Plateau, using air temperature in the highest available pressure of MOD07 as $T_a$would generate systematic underestimation. Hydrolytical interpolation to surface pressure level can greatly improve the air temperature retrieval quality, while hypsometrical interpolation only obtains slight improvement because of the largely introduced outliers. Clouds may also have a pronounced impact on the accuracy of these methods because of the parabola-like error distribution in low elevation areas. In contrast, by combining the underestimates of hydrostatic interpolation with the overestimation from land surface temperature, good performance can be achieved in both low and high elevation areas. The results from this study can provide important references for future use of air temperature derived from satellite data and potentially improve the global models ranging from climatology, hydrology to ecology.

CRediT authorship contribution statement

Wenjie Zhang, Baiping Zhang and Wenbin Zhu designed the study. Wenjie Zhang conducted the analysis and wrote the manuscript. Wenbin Zhu, Xiaolu Tang, Fujie Li, Xisheng Liu and Qiang Yu interpreted the results and revised the manuscript.

Funding

This study was supported by research grants from the National Natural Sciences Foundation of China (42071032 and 41601478), the Key Science and Technology Project of Qinghai Province (2019-SF-A4), the Basic Research Program of Qinghai Province (2020-ZJ-715), and Youth Innovation Promotion Association of Chinese Academy of Sciences (2020056).

Declaration of competing interest

The authors declare no competing interests.

Acknowledgements

We are highly grateful to the MODIS mission scientists and associated NASA personnel for their data support. We also thank the anonymous reviewers for their comments and suggestions that improved this paper.

References

Benali, A., Carvalho, A., Nunes, J., Carvalhais, N., Santos, A., 2012. Estimating air surface temperature in Portugal using MODIS LST data. Remote Sens. Environ. 124, 108–121.

Bisht, G., Bras, R., 2010. Estimation of net radiation from the MODIS data under all sky conditions: southern Great Plains case study. Remote Sens. Environ. 114 (7), 1522–1534.

Bisht, G., Venturini, V., Islam, S., Jiang, L., 2005. Estimation of the net radiation using MODIS (Moderate resolution imaging Spectroradiometer) data for clear sky days. Remote Sens. Environ. 97 (1), 52–67.

Borbas, E., Suzanne Seemann, W., Huang, H., Li, J., Paul Menzel, W., 2005. Global profile training database for satellite regression retrievals with estimates of skin temperature and emissivity. Proceedings of the XIV, International ATOVS Study Conference, Beijing, China. University of Wisconsin-Madison, Space Science and Engineering Center, Cooperative Institute for Meteorological Satellite Studies (CIMSS), Madison, WI, pp. 763–770 (2005).

Buermann, W., Forkel, M., O'Sullivan, M., Sitch, S., Friedlingstein, P., Haverd, V., Jain, A., Kato, E., Kautz, M., Lienert, S., 2018. Widespread seasonal compensation effects of spring warming on northern plant productivity. Nature 562 (7725), 110.

Cai, D., You, Q., Fraedrich, K., Guan, Y., 2017. Spatiotemporal temperature variability over the tibetan plateau: altitudinal dependence associated with the global warming hiatus. J. Clim. 30 (3), 969–984.

Collados-Lara, A., Fassnacht, S., Pardo-Igúzquiza, E., Pulido-Velazquez, D., 2021. Assessment of high resolution air temperature fields at rocky mountain national park by

combining scarce point measurements with elevation and remote sensing data. Remote Sens. 13, 113 (2021).
Cristóbal, J., Ninyerola, M., Pons, X., 2008. Modeling air temperature through a combination of remote sensing and GIS data. J. Geophys. Res. Atmos. 113 (D13).
Famiglietti, C., Fisher, J., Halverson, G., Borbas, E., 2018. Global validation of MODIS near-surface air and dew point temperatures. Geophys. Res. Lett. 45 (15), 7772–7780.
Flores, F., Lillo, M., 2010. Simple air temperature estimation method from MODIS satellite images on a regional scale. Chil. J. Agric. Res. 70 (3), 436–445.
Geiger, R., 1965. The Climate Near the Ground Harvard University Press, Massachusetts, Cambridge.
Golkar, F., Sabziparvar, A., Khanbilvardi, R., Nazemosadat, M., Zand-Parsa, S., Rezaei, Y., 2018. Estimation of instantaneous air temperature using remote sensing data. Int. J. Remote Sens. 39 (1), 258–275.
Goward, S., Waring, R., Dye, D., Yang, J., 1994. Ecological remote sensing at OTTER: satellite macroscale observations. Ecol. Appl. 4 (2), 322–343.
Hu, L., Brunsell, N., 2015. A new perspective to assess the urban heat island through remotely sensed atmospheric profiles. Remote Sens. Environ. 158, 393–406.
Jang, K., Kang, S., Lim, Y., Jeong, S., Kim, J., Kimball, J., Hong, S., 2013. Monitoring daily evapotranspiration in Northeast Asia using MODIS and a regional land data assimilation system. J. Geophys. Res. Atmos. 118 (23), 12927–12940.
Jang, K., Kang, S., Kimball, J., Hong, S., 2014. Retrievals of all-weather daily air temperature using MODIS and AMSR-E data. Remote Sens. 6 (9), 8387–8404.
Kim, J., Hogue, T., 2008. Evaluation of a MODIS-based potential evapotranspiration product at the point scale. J. Hydrometeorol. 9 (3), 444–460.
Lin, S., Moore, N., Messina, J., DeVisser, M., Wu, J., 2012. Evaluation of estimating daily maximum and minimum air temperature with MODIS data in East Africa. Int. J. Appl. Earth Obs. Geoinf. 18, 128–140.
Liu, S., Su, H., Tian, J., Zhang, R., Wang, W., Wu, Y., 2017. Evaluating four remote sensing methods for estimating surface air temperature on a regional scale. J. Appl. Meteorol. Climatol. 56 (3), 803–814.
Liu, Q., Piao, S., Janssens, I., Fu, Y., Peng, S., Lian, X., Ciais, P., Myneni, R., Peñuelas, J., Wang, T., 2018. Extension of the growing season increases vegetation exposure to frost. Nat. Commun. 9 (1), 426.
Monteith, J., 1973. Principles of Environmental Physics Edward Arnold. 214p. .
Mostovoy, G., King, R., Reddy, K., Kakani, V., Filippova, M., 2006. Statistical estimation of daily maximum and minimum air temperatures from MODIS LST data over the state of Mississippi. GISci. Remote Sens. 43 (1), 78–110.
Nieto, H., Sandholt, I., Aguado, I., Chuvieco, E., Stisen, S., 2011. Air temperature estimation with MSG-SEVIRI data: calibration and validation of the TVX algorithm for the Iberian Peninsula. Remote Sens. Environ. 115 (1), 107–116.
Østby, T., Schuler, T., Westermann, S., 2014. Severe Cloud Contamination of MODIS Land Surface Temperatures Over an Arctic Ice Cap, Svalbard. 142, pp. 95–102.
Oyler, J., Dobrowski, S., Holden, Z., Running, S., 2016. Remotely sensed land skin temperature as a spatial predictor of air temperature across the conterminous United States. J. Appl. Meteorol. Climatol. 55 (7), 1441–1457.
Peón, J., Recondo, C., Calleja, J., 2014. Improvements in the estimation of daily minimum air temperature in peninsular Spain using MODIS land surface temperature. Int. J. Remote Sens. 35 (13), 5148–5166.
Prihodko, L., Goward, S., 1997. Estimation of air temperature from remotely sensed surface observations. Remote Sens. Environ. 60 (3), 335–346.
Prince, S., Goetz, S., Dubayah, R., Czajkowski, K., Thawley, M., 1998. Inference of surface and air temperature, atmospheric precipitable water and vapor pressure deficit using advanced very high-resolution radiometer satellite observations: comparison with field observations. J. Hydrol. 212, 230–249.
Ryu, Y., Baldocchi, D., Kobayashi, H., Van Ingen, C., Li, J., Black, T., Beringer, J., Van Gorsel, E., Knohl, A., Law, B., 2011. Integration of MODIS land and atmosphere products with a coupled-process model to estimate gross primary productivity and evapotranspiration from 1 km to global scales. Glob. Biogeochem. Cycles 25 (4), 1–24.
Seddon, A., Macias-Fauria, M., Long, P., Benz, D., Willis, K., 2016. Sensitivity of global terrestrial ecosystems to climate variability. Nature 531 (7593), 229.
Sellers, P., Dickinson, R., Randall, D., Betts, A., Hall, F., Berry, J., Collatz, G., Denning, A., Mooney, H., Nobre, C., 1997. Modeling the exchanges of energy, water, and carbon between continents and the atmosphere. Science 275 (5299), 502–509.
Shen, S., Leptoukh, G., 2011. Estimation of surface air temperature over central and eastern Eurasia from MODIS land surface temperature. Environ. Res. Lett. 6 (4), 045206.
Sims, D., Rahman, A., Cordova, V., El-Masri, B., Baldocchi, D., Flanagan, L., Goldstein, A., Hollinger, D., Misson, L., Monson, R., 2006. On the use of MODIS EVI to assess gross primary productivity of north American ecosystems. J. Geophys. Res. Biogeosci. 111 (G4).
Sobrino, J., Jiménez-Muñoz, J., Mattar, C., Sòria, G., 2015. Evaluation of Terra/MODIS atmospheric profiles product (MOD07) over the Iberian Peninsula: a comparison with radiosonde stations. Int. J. Digital Earth 8 (10), 771–783.
Stisen, S., Sandholt, I., Nørgaard, A., Fensholt, R., Eklundh, L., 2007. Estimation of diurnal air temperature using MSG SEVIRI data in West Africa. Remote Sens. Environ. 110 (2), 262–274.
Sun, Y., Wang, J., Zhang, R., Gillies, R., Xue, Y., Bo, Y., 2005. Air temperature retrieval from remote sensing data based on thermodynamics. Theor. Appl. Climatol. 80 (1), 37–48.
Vancutsem, C., Ceccato, P., Dinku, T., Connor, S., 2010. Evaluation of MODIS land surface temperature data to estimate air temperature in different ecosystems over Africa. Remote Sens. Environ. 114 (2), 449–465.
Verma, M., Fisher, J., Mallick, K., Ryu, Y., Kobayashi, H., Guillaume, A., Moore, G., Ramakrishnan, L., Hendrix, V., Wolf, S., 2016. Global surface net-radiation at 5 km from MODIS Terra. Remote Sens. 8 (9), 739.
Xie, X., He, B., Guo, L., Miao, C., Zhang, Y., 2019. Detecting hotspots of interactions between vegetation greenness and terrestrial water storage using satellite observations. Remote Sens. Environ. 231, 111259.
Zhang, J., Gao, S., Chen, H., Yu, J., Tang, Q., 2015. Retrieval of the land surface-air temperature difference from high spatial resolution satellite observations over complex surfaces in the Tibetan plateau. J. Geophys. Res. Atmos. 120 (16), 8065–8079.
Zhang, W., Zhou, T., Zhang, L., 2017. Wetting and greening Tibetan plateau in early summer in recent decades. J. Geophys. Res. Atmos. 122 (11), 5808–5822.
Zhu, W., Lu, A., Jia, S., 2013. Estimation of daily maximum and minimum air temperature using MODIS land surface temperature products. Remote Sens. Environ. 130, 62–73.
Zhu, W., Jia, S., Lu, A., 2017a. A universal Ts-VI triangle method for the continuous retrieval of evaporative fraction from MODIS products. J. Geophys. Res. Atmos. 122 (19), 10,206–210,227.
Zhu, W., Lu, A., Jia, S., Yan, J., Mahmood, R., 2017b. Retrievals of all-weather daytime air temperature from MODIS products. Remote Sens. Environ. 189, 152–163.
Zveryaev, I.I., Zahn, M., Allan, R.P., 2016. Interannual variability in the summertime hydrological cycle over European regions. J. Geophys. Res. Atmos. 121 (10), 5381–5394.